Supporting Information

Colombo *et al.* 10.1073/pnas.0802879105

SI Text

Molecular Dynamics of Hsp90 Complexes. Long time scale all-atom molecular dynamics (MD) simulations in explicit water, with simulation times of at least 70 ns have been independently carried out with the GROMACS software package (1), using the GROMOS96 force field (2, 3) and the SPC water model (4) on the structures of the complexes described in the text. Each complex was first energy relaxed with the 2,000 steps of steepest descent energy minimization followed by another 2,000 steps of conjugate gradient energy minimization. The energy minimization was used to remove possible bad contacts from the initial structures. For each of conducted simulations, the system was equilibrated by 50 ps of MD runs with position restraints on the protein and ligand to allow relaxation of the solvent molecules. These first equilibration runs were followed by other 50-ps runs without position restraints on the solute. The first 15 ns of each trajectory were not used in the subsequent analysis to minimize convergence artifacts (Fig. S7). Equilibration of the trajectories was checked by monitoring the equilibration of quantities such as the RMSD with respect to the initial structure, internal protein energy, fluctuations calculated on different time-intervals. The electrostatic term was described by using the particle mesh Ewald algorithm. In each explicit solvent simulation, the temperature and pressure were kept to the desired value by weak coupling to an external bath (T = 300 K, τ_T 0.1 ps; P_0 = 1 bar, coupling time τ_P = 0.5 ps) (5). The production runs for the different complexes, after equilibration, covered the following time scales: 100 ns for apo-Hsp90; 70 ns for ADP/Hsp90; 70 ns for ATP/Hsp90; 70 ns for Shepherdin/Hsp90; 70 ns for Shepherdin[79–83]/Hsp90; and 100 ns for the AICAR/Hsp90 complex. Representative conformations from each simulation were selected by applying the cluster analysis method developed in (6). Molecular dynamics simulations of the apo Hsp90 NTD were subsequently performed for an additional 200 ns, using parallel version of the program NAMD 2.6. An NPT ensemble was used, and periodic boundary conditions were imposed on the systems. The nonbonded cutoff, switching distance, and nonbonded pair-list distance were set to 9, 8, and 10.5 Å, respectively. Constant pressure and temperature on the system were maintained with an isotropic Langevin barostat and a Langevin thermostat. Thousand steps of conjugate gradient algorithm were used to minimize each system with restraints to protein backbone, followed by 1,000 steps without restraints. The system was warmed up for 40 ps and equilibrated for 100 ps with lower restraints, finishing with no restraints at 300 K.

Molecular Docking. The same docking protocols have been followed to generate all of the Hsp90-inhibitor complexes described in this study. The detailed docking procedures have been described for Shepherdin in ref 7, for minimal peptides in ref. 8, and for AICAR in ref. 9 and in its supplementary material. Briefly, the docking procedure can be summarized as follows: the representative conformations obtained from the statistical cluster analysis of long timescale MD simulations for each ligand were subjected to blind docking experiments on the putative N-terminal Hsp90 receptor, using the program AutoDock (10). The crystal structure of the protein was taken from the protein data bank (PDB entry 1YET) (11). The original x-ray structure contains the ligand GA, which was removed from the active site to yield the apo-open form of Hsp90.

Essential Dynamics Analysis and Dynamics Similarity Metrics. In this work, for each of the simulated complexes the covariance matrix of the Hsp90 NTD was built by averaging motions of Cα atoms deviating from the mean structure, with the latter calculated over the trajectory excluding the first 15 ns needed for equilibration. Ligands were not included in the calculation. Translational and rotational degrees of freedom are eliminated and the average atomic coordinates, $x_{i,ave}$, are calculated along the MD trajectory (12). The essential directions of correlated motions during dynamics were then calculated by diagonalizing the covariance matrix C_{ij}.

$$C_{ij} = \langle (x_i - x_{i,ave})(x_j - x_{j,ave}) \rangle$$

By projecting the MD trajectory onto the main essential direction, corresponding to the largest eigenvector, one can visualize the extreme structures and the major fluctuations of the correlated motions.

1. van der Spoel D, *et al.* (2004) *Gromacs User Manual Version 3.2.* Available at www.gromacs.org.
2. van Gunsteren WF, Berendsen HJC (1987) GROMOS (GROningen MOlecular Simulation package) (Biomos BV, The Netherlands).
3. van Gunsteren, *et al.* (2006) Biomolecular modeling: Goals, problems, perspectives. *Angew Chem Int Ed* 45:4064–4092.
4. Berendsen HJC, Grigera JR, Straatsma PR (1987) The missing term in effective pair potentials. *J Phys Chem* 91:6269–6271.
5. Berendsen HJC, Postma JPM, van Gunsteren WF, Di Nola A, Haak JR (1984) *J Chem Phys* 81:3684–3690.
6. Daura X, Jaun B, Seebach D, van Gunsteren WF, Mark AE (1998) *J Mol Biol* 280:925–932.
7. Plescia J, *et al.* (2005) *Cancer Cell* 7:457–467.
8. Gyurkocza B, *et al.* (2006) *J Natl Cancer Inst* 98:1068–1077.
9. Meli M, *et al.* (2006) *J Med Chem* 49:7721–7730.
10. Morris GM, *et al.* (1998) *J Comput Chem* 19:1639–1662.
11. Stebbins CE, *et al.* (1997) *Cell* 89:239–250.
12. Amadei A, Linssen ABM, Berendsen HJC (1993) *Proteins Struct Funct Genet* 17:412–425.

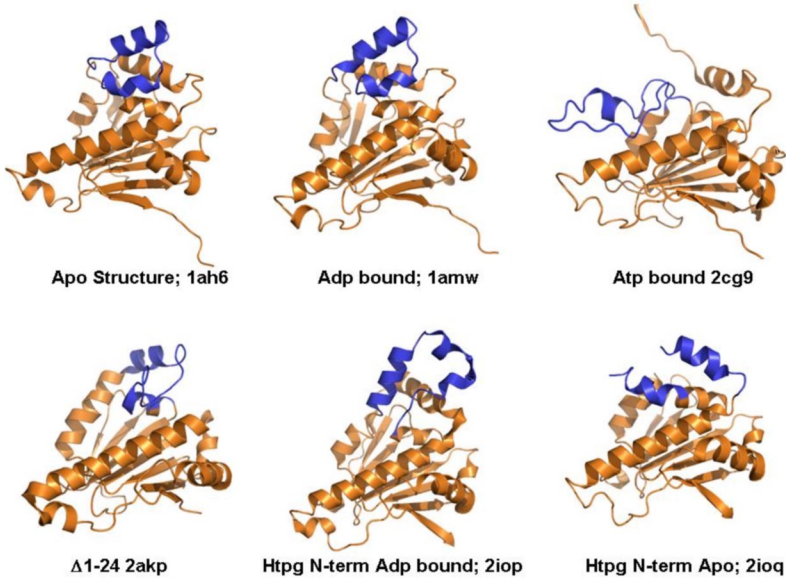

Fig. S1. The crystal structures of the Hsp90 NTD. The ATP lid is highlighted in blue. These structures represent several apo and ADP complexes of the isolated Hsp90 NTD. The structure labeled 2cg9.pdb is obtained from the full-length dimer structure in the complex with an ATP mimic and illustrates the closed conformation of the ATP-lid in the context of the functional dimer. The conformational changes seen in the crystal structures involve lid on passing from the apo or ADP complex to the situation in the dimer.

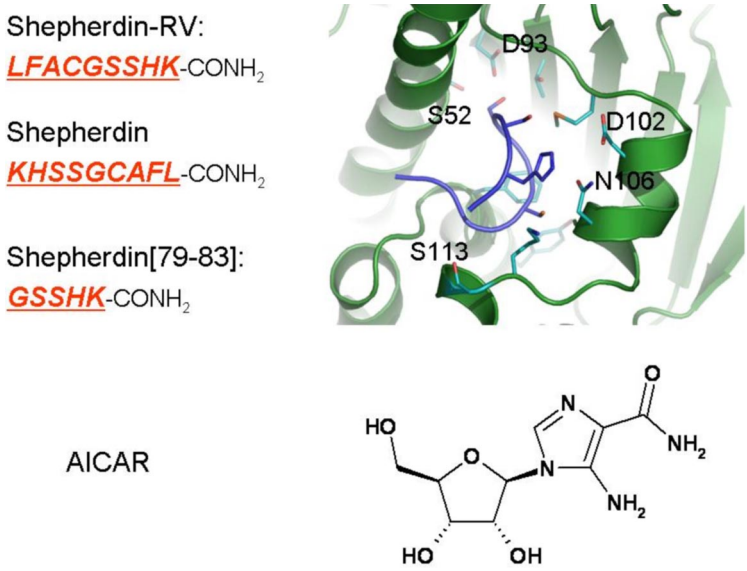

Fig. S2. Sequences of Shepherdin, Shepherdin-RV, and Shepherdin[79–83], and the chemical structure of AICAR.

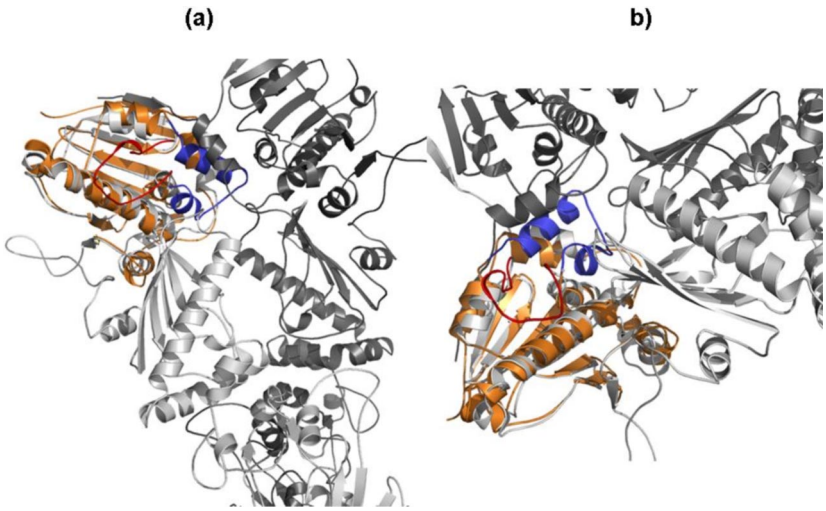

Fig. S3. Comparison of the 3D structure of the inhibitor bound Hsp90 NTD with the structure of the NTD in full-length dimer. (*a*) Superposition of the representative structure of the Shepherdin-Hsp90 NTD complex (orange structure; the ATP-lid is shown in blue) with the corresponding N-domain in the context of the full-length dimeric structure obtained from x-ray spectroscopy [PDB entry 2CG9 (14)] (light gray, protomer 1; red, ATP-lid; dark gray, protomer 2). (*b*) Magnified view of the same superposition. It is apparent that the ATP-lid conformation (blue ribbon) in the Shepherdin-Hsp90 NTD complex would lead to severe steric clashes with helix 1 from the NTD of the second protomer (dark gray) and with several loops shaping the interface in the formation of the full-length functional dimer. In the dimer, the ATP-lid adopts a different conformation (red), avoiding unfavorable contacts. Motion of the ATP-lid in the ATP-Hsp90 NTD complex described in the text minimizes the steric clashes.

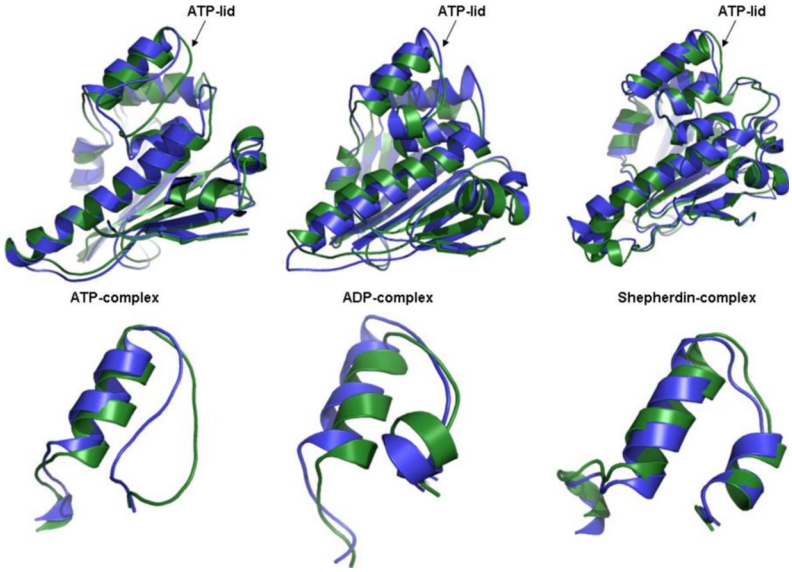

Fig. S4. The two most different structures, extreme structures, obtained from the projection of the trajectory on the respective principal component. The ATP-lid is highlighted in the lower panel. Conformational differences are evident in the ATP-lid region upon ligand variation.

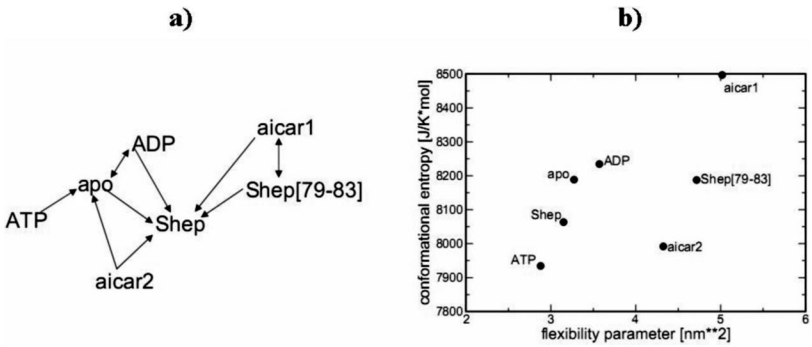

Fig. S5. Topological similarity of Hsp90-substrate dynamical subspaces. (*a*) The complexes clustered according to the similarities based on the RWSIP metric. Arrows connect each complex with the two other complexes sharing the most similar essential conformational subspaces. (*b*) Flexibility–entropy correlation for all of the complexes. The entropy for each domain is calculated by using the Schlitter's formula.

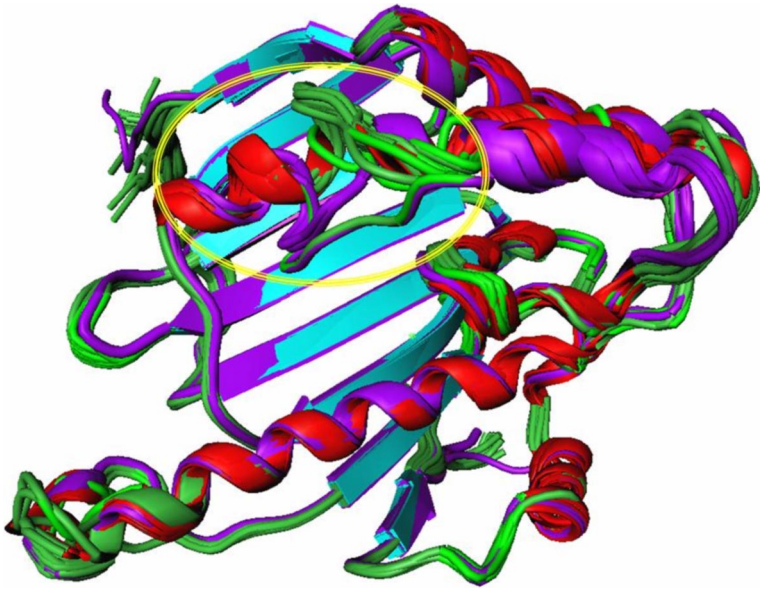

Fig. S6. The representative snapshots from the 200 ns long implicit solvent simulation of Hsp90 NTD with no ligand bound. The circle focuses on the degree of the lid remodeling in simulations.

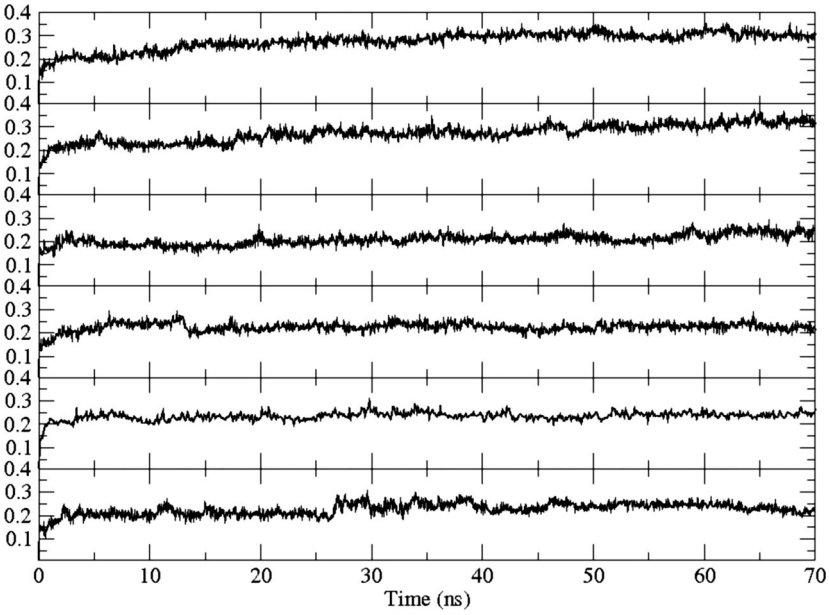

Fig. S7. Time evolution of the root mean square deviation (rmsd) from the initial structure of the protein in the simulations.

Table S1. Values of the root weighted mean square inner product (RWSIP) (described in *Materials and Methods*) calculated by comparing the essential subspaces of pairs of simulations

RWSIP	APO	ATP	ADP	AICAR1	AICAR2	Shepherdin
ATP	0.412	—	—	—	—	—
ADP	0.461	0.389	—	—	—	—
AICAR1	0.456	0.363	0.409	—	—	—
AICAR2	0.493	0.347	0.400	0.381	—	—
Shepherdin	0.521	0.496	0.459	0.492	0.504	—
Shepherdin79–83	0.380	0.364	0.390	0.512	0.350	0.464

Table S2. Neighbor list containing the two complexes with the most similar and the two with the most different conformational subspaces

Complex	Close	Distant
ATP	Shepherdin, APO	AICAR1, AICAR2
APO	Shepherdin, AICAR2	Shepherdin79–83, ATP
ADP	APO, Shepherdin	ATP, Shepherdin79–83
Shepherdin	APO, AICAR2	ADP, Shepherdin79–83
Shepherdin79–83	AICAR1,Shepherdin	AICAR2, ATP
AICAR1	Shepherdin7983,Shepherdin	ATP, AICAR2
AICAR2	Shepherdin, APO	ATP, Shepherdin79–83

Table S3. Global flexibility and configurational entropy calculated from the covariance matrices

Complex	Flexibility	Entropy, J/K·mol
ATP	2.87883	7,934.48
APO	3.27236	8,188.59
ADP	3.57119	8,234.59
Shepherdin	3.14891	8,063.52
Shepherdin79–83	4.71716	8,187.47
AICAR1	5.01787	8,496.95
AICAR2	4.32398	7,991.95